BOLLETTINO DI GEOFISICA TEORICA ED APPLICATA VOL. XXXIII, N. 132 - DECEMBER 1991

A. BOTTARI [1], P. CARVENI [2], M. PIETRAFESA [1] and E. STILLITANI [1]

METHODOLOGICAL PROBLEMS IN SEISMIC HAZARD EVALUATION FOR THE NORTH-EASTERN SICILY AREA

Abstract. An analysis of seismic hazard was carried out in northeaster Sicily using a program derived from McGuire's procedure, later modified by Saeggesser and Mayer Rosa, for the twin purposes of examining its adaptability to the area of interest and finding its efficiency and limits. On the basis of tests carried out, the main uncertainties in the evaluation of seismic hazard are shown to derive from the degree of subjectivity and from the lack of historical information on the choice and quantification of input parameters. The latter was examined by tests using various combinations of input parameters. The data used were taken from the Catalogue of Italian Earthquakes, assuming V MCS as intensity threshold. The maps of expected maximum intensities produced for return periods between 50 and 500 years, corresponding to different input combinations, show much lower values with respect to the historical maximum observed in the area. This prompted an in depth analysis to redetermine the main input parameters which influence the projection of the expected maximum intensities.

INTRODUCTION

Characterization of the expected maximum intensity value distribution in a given area is the main aim of a seismic hazard analysis.

Calculation of the projection values was done using the McGuire calculation code (1976) in the version modified by Saeggesser and Mayer-Rosa (1978).

For optimization of the results, careful preparation of the input parameters is necessary. The uncertainty in the calculations and subjectivity in the choices made influence the input parameters. This follows from critical observations on results from different areas of investigation (Barbano et al., 1986; Barbano et al., 1989b). Furthermore, the evaluation of hazard is bound to a correct geologic-structural interpretation of the area generating the "historical" seismicity and assumed as a "cognitive window". This has been seen in the surveys carried out for the areas most at risk in the national territory (Barbano et al., 1988; Slejko and Siro, 1988; Barbano et al., 1989a; Siro and Slejko, 1989).

For the optimization of the results, it seemed opportune to quantify the "weight" of each input parameter on the projection values. This is the main aim of the survey which was carried out as a series of tests, each characterized by the use of a different combination of input parameters to the calculation code. Thus modifications were made to the size (variation up to 40%) and the geometry of the source zones (different and diversely oriented quadrilaterals, compatible with the tectonic structures), to the maximum observed intensities and the relative error for each, and to the attenuation coefficients for each source zone.

A comparison of the maps of maximum expected intensity for each combination of inputs

Manuscript received August 21, 1991; accepted December 1, 1991.

[1] Istituto Geofisico e Geodetico, University, via Osservatorio 4, 98121 Messina, Italy.

[2] Istituto di Scienze della Terra, University, corso Italia 55, 95100 Catania, Italy.

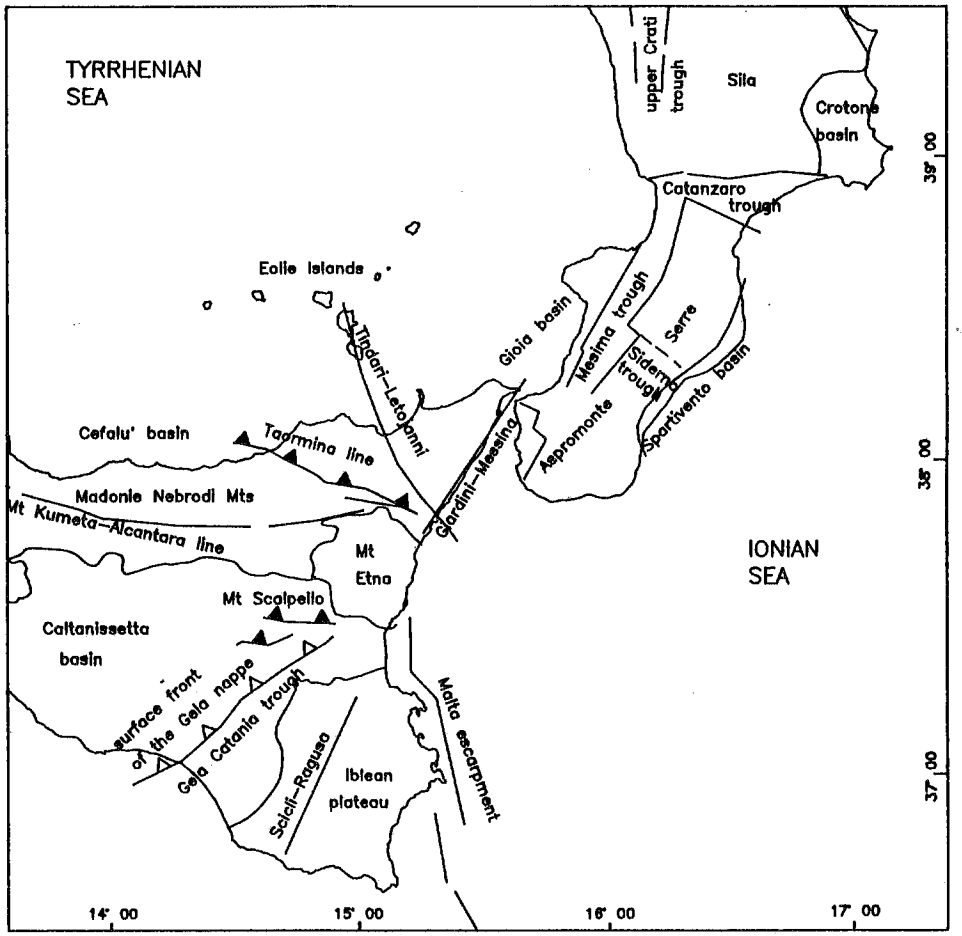

Fig. 1 - Map of the most important tectonic structures present in the region analysed, following the Ghisetti and Vezzani (1982) scheme.

highlights the influence of each parameter on the projection values.

STRUCTURAL OUTLINE

From a geodynamical point of view, the Calabro-Peloritan Arc consitutes one of the most interesting areas in Italy. It acts as a "hinge" between the African and Eurasian plates.

The most important active tectonic structures (Fig. 1) are located along fault systems oriented parallel to the Apenine chain, or ortogonally to it. In Southern Calabria, the first group is represented by distensive faults partly located along the continental escarpment of the Tyrrhenian sea with a general NNE-SSW direction and with a draw pulling of the western edge and which, to the west, delimits the upper structures of Cape Vaticano, the Serre, and Aspromonte; the faults which give origin to the tectonic trough of the river Mesima, and those which border the Ionic margin of Calabria with a prevalently NE-SW direction are part of the same tectonic system.

Along the north coast of Sicily, this system is formed by the alignment of faults with an ENE-WSW direction between Cape Rasocolmo and the Cape Tindari area, and with a NE-SW direction and E-W direction from Cape d'Orlando to S. Stefano di Camastra. In a more external position, a series of normal right strike-slip faults in an E-W direction separates the coa-

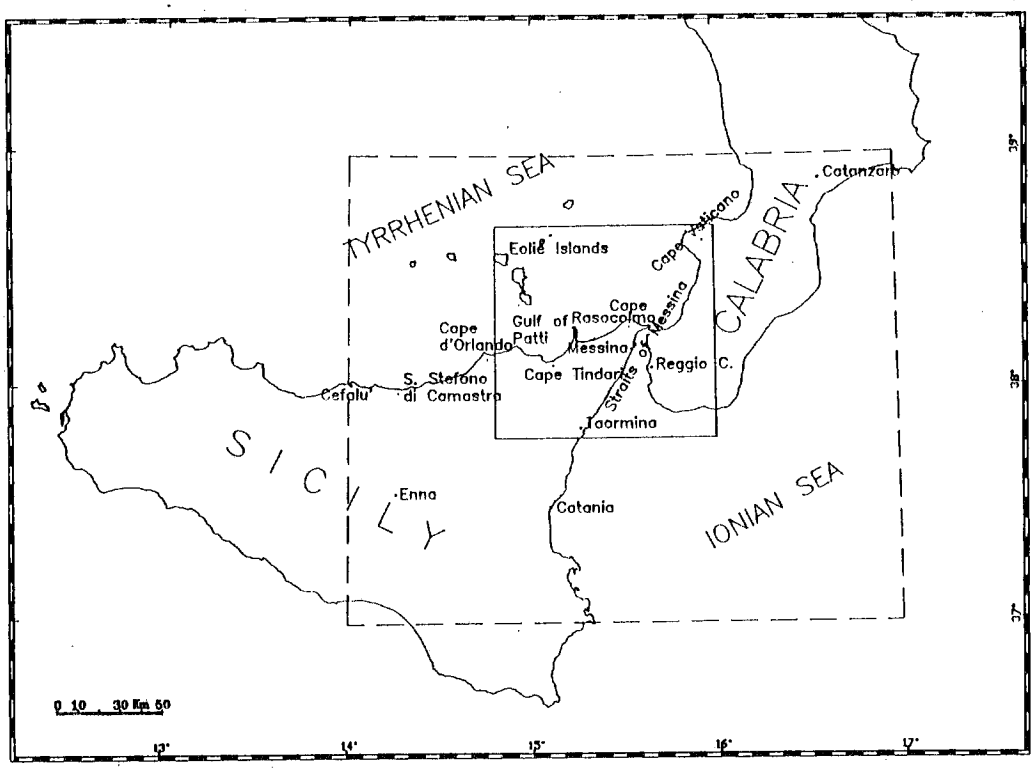

Fig. 2 - Graphic representation of the "window" of territory analysed (delimited by the dotted line) and of the area of interest for the intensity projection (delimited by continuous line).

stal chain from the Caltanisetta basin to the south. Even more externally, a series of normal faults of direction NE-SW causes the downstep of the coastal chain and creates small columns and tectonic troughs.

The second group is formed by alignments of direct faults which cause the formation of tectonic troughs with a transversal direction in Calabria. These are more open along the Ionian coastline with respect to the Tyrrhenian (tectonic troughs of Catanzaro, Siderno, the Messina Straits). In north-east Sicily the alignments of Messina-Giardini, with a NNE-SSW direction and right strike-slip movement, and the alignment Tindari-Letojanni, with a NW-SE direction and right stike-slip movement, both belong to this group. Another important tectonic structure is formed by the fault system of the Ibleo-Maltese escarpment which develops in a NNW-SSE direction and conditions the seismicity of the south-eastern sector of the island and the eastern Etnean side.

The structures of Mount Etna, which show frequent seismic activity, although of medium intensity, are also included in the complex tectonic framework characterized here.

INVESTIGATION METHOD

The intensity projection obtained is relative to an area surrounding the Straits of Messina, from the Gulf of Patti to Reggio Calabria. A study of seismic hazard requires however, a seismicity analysis of a 'window' of wider territory than the area of interest. Thus the area geographically delimited by the parallels 37° 00' - 39° 00' N, and the meridians 14° 00' - 17° 00' E (Fig. 2) was chosen.

The data used for the analysis were taken from the Catalogue of Italian Earthquakes

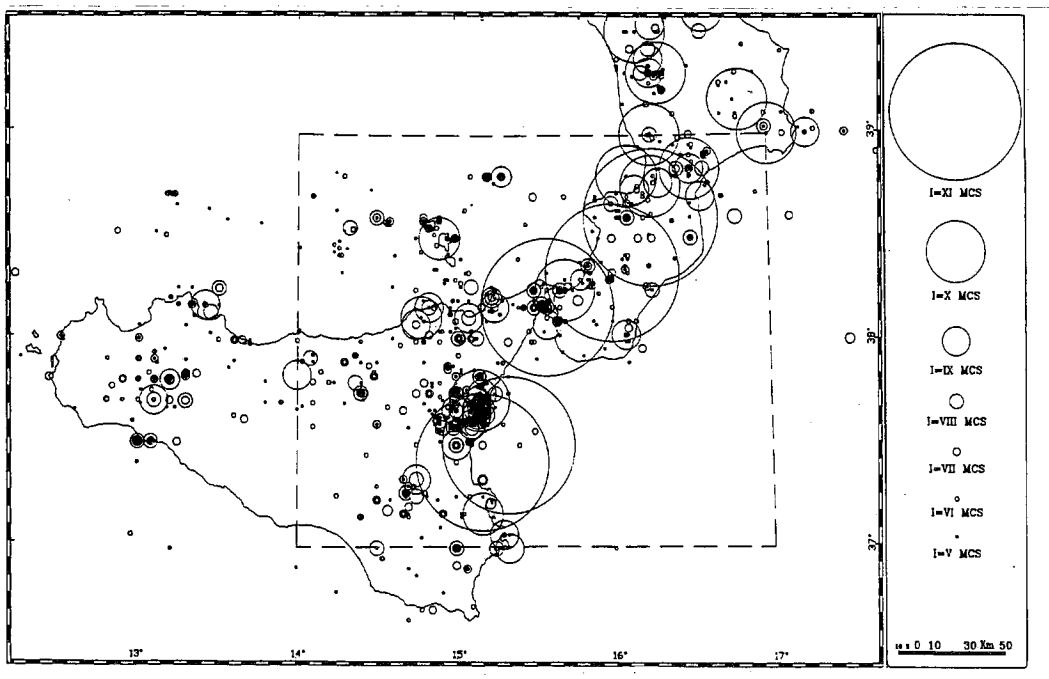

Fig. 3 - Epicentral map of events $I_0 \geq$ V MCS inside the window of investigation, from 1000 to 1980. Each event is represented by a circle of radius proportional to the focal volume according to the Bath and Duda (1964) relationship.

(Postpischl, 1985) and are relative to seismic events having a maximum epicentral intensity $I_0 \geq$ V MCS, and epicentres inside the "window" previously defined (Fig. 3). The choice of threshold value V MCS meets two requirements: the first is to have for the lower limit of seismic intensity analysed a value which is still important in terms of hazard (V MCS is characterized by an intensity just below the limit of damage to buildings); the second is to obtain a sufficiently complete data set over a sufficiently long period of time. From analyses of completeness carried out on the Catalogue, time intervals of 180, 250, 350 and 500 years (Table 1) proved to be reliable (Fig. 4); the interval $\Delta t \approx$ 180 years was, howerver, chosen in order to privilege the quality of the "historical" data.

The areal distribution of epicentres follows the trend of the major tectonic structures, allowing the definition of four source zones (Fig. 5a). The first (ZS1) extends from ghe Catanzaro graben as far as the Straits of Messina, and is to be identified with the territory of the Calabro-Peloritan Arc, while the second (ZS2) includes the territory between the Eolian islands, the Nebrodi mountains, part of the Peloritans chain and the most northerly part of the Tindari-

Table 1 - Number of events along different time periods for the investigated area.
The events are grouped according to intensity.

T (YRS)	1800-1980	1730-1980	1630-1980	1480-1980
I (MCS)	N	N	N	N
V	940	1162	1180	1181
VI	308	383	407	415
VII	153	195	217	232
VIII	39	51	62	69
IX	11	16	19	24
X	4	6	8	8
XI	1	3	4	4

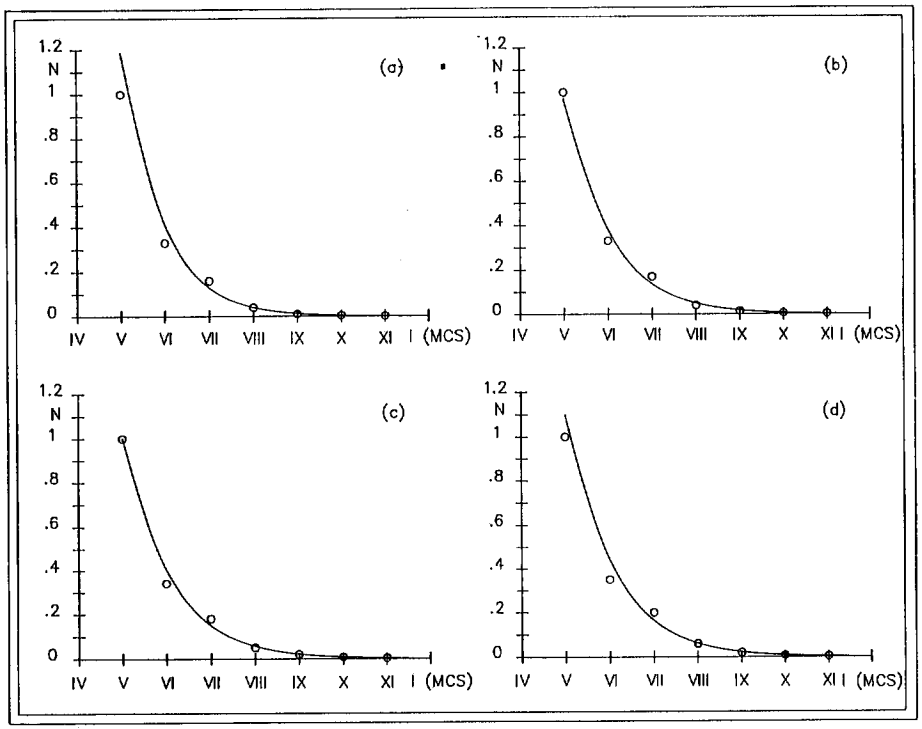

Fig. 4 - Graphic representation of Catalogue completeness for different time periods. From 1800 to 1980 (T=180 years) (a); from 1730 to 1980 (T=250 years) (b); from 1630 to 1980 (T=350 years) (c); from 1480 to 1980 (T=500 years) (d). All functions are normalized. The data sets are listed in Table 1.

Letojanni fault line. The third (ZS3), less extensive, involves the Etnean area, and the fourth (ZS4), the most southerly, delimits the northern part of the Iblean area.

The source zones are characterized by different seismicity trends. The histograms of Fig. 6 show the seismic distribution for each source zone relative to the period (1000 years) covered by the Catalogue (Postpischl, 1985). In particular, as shown in Table 2, the Calabro-Peloritan area (Zone ZS1) shows the highest number of events of the four zones considered, and the maximum intensity (3 events of XI MCS). ZS2 and ZS3 show intermediate values for the number of events and maximum intensity not greater than X MCS. ZS4 is characterized by a rather low number of events of medium intensity (V MCS), and by a higher percentage (relative to the other source zones) of medium-high intensity events (1 event of intensity XI MCS).

The average hypocentral depth for source zones ZS1, ZS2 and ZS4 from previous macroseismic studies carried out in the same area (Bottari et al., 1979) is estimated at about 20 km, while that of ZS3 is more superficial (about 7 km) and is also associated with events of volcanic origin.

The importance of a correct definition of the source zones on the intensity projection prompted us to test variations of size and direction in order to quantify the "weight" of their geometry.

Table 2 - Number of events over 1000 years for each source zone.
The events are grouped according to intensity.

ZS	V	VI	VII	VIII	IX	X	XI
1	511	212	102	19	5	3	3
2	75	30	13	10	6	0	0
3	380	108	65	18	6	1	0
4	31	13	14	7	4	0	1

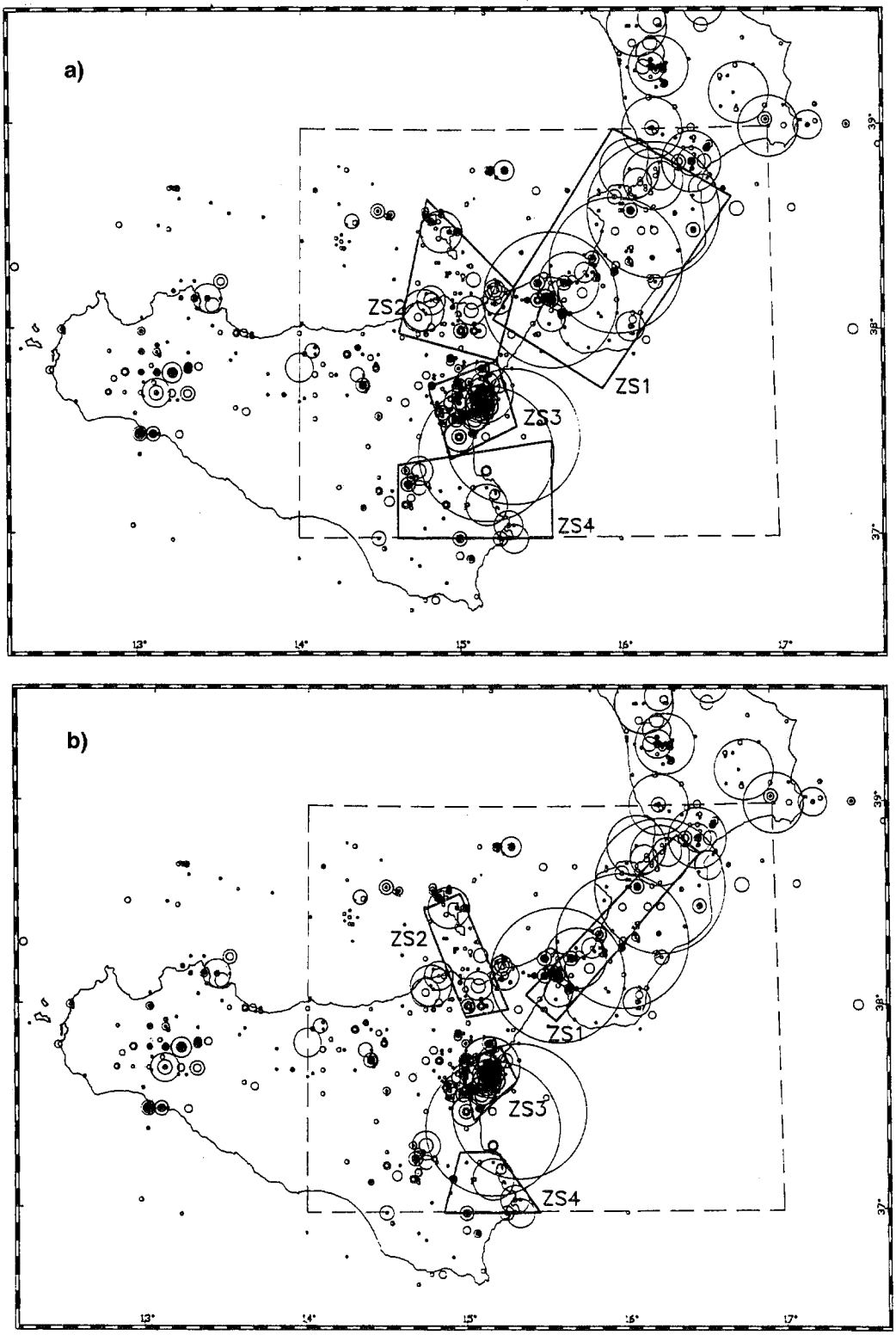

Fig. 5 - Representation of the source zones in relation to epicentral distribution: a) maximum extension considered for each ZS; b) size of the ZS reduced by 40% with respect to the previous but with unvaried orientation; c) configuration of the ZS as before in terms of extension, but the orientation of ZS2 and the form of ZS3 vary.

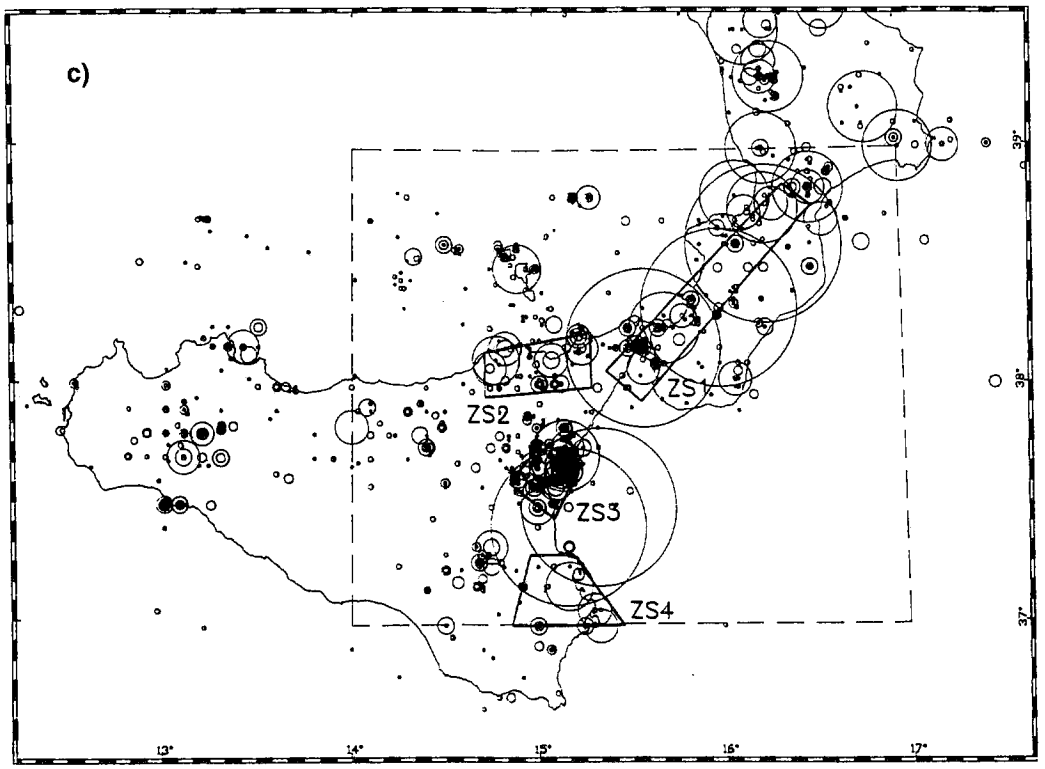

Fig. 5 - Continued.

Thus two other different configurations of source zones were adopted (Figs. 5a, 5b, 5c), limiting the size (to about 40% of the starting value) and varying the direction compatibly with that of the tectonic structures in the area examined. In particular, size reduction of the source zones was done to find a configuration corresponding better to the real geometry of the active seismotectonic structures and to the real configuration of the focal volumes and, at the same time, to quantify the influence of size on the intensity projections. Regarding the variations in directions, which involve exclusively ZS2, two preferential directions were chosen: NNW-SSE compatible with the direction of the Tindari-Letojanni fault line (Fig. 5b), and E-W transversal to it (Fig. 5c).

Other tests carried out consisted in the variation of other input parameters, such as the maximum historical intensity observed for each ZS, the uncertainty in the evaluation of the intensity, and the attenuation coefficients of the macroseismic intensity. The first test was characterized by the most optimistic conditions: for the maximum intensity of each source area, the historically observed value was assumed by attributing the value zero to the standard deviation of the normal distribution; this was equivalent to considering the historical information as exact. In order to take into account the uncertainty in the historical intensity values, two different tests were carried out: one by assuming the values 0.5 and 1.0 for the standard deviation of the normal distribution. The second by increasing the historical values by one unit. The different combinations of these parameters form the different input files to the code.

The attenuation of intensity for each ZS in the program is modelled according to the Koveslighety-Sponheuer law (Sponheuer, 1960). In order to show the different degrees of attenuation between the near-field and the far-field, two values of coefficient α were identified for the two maximum and minimum attenuation directions, one relative to the near-field ($I_o \geq$ VIII MCS) and one to the far-field ($I_o <$ VIII MCS), by introducing suitable modifications to the original program (Saeggesser and Mayer-Rosa, 1978).

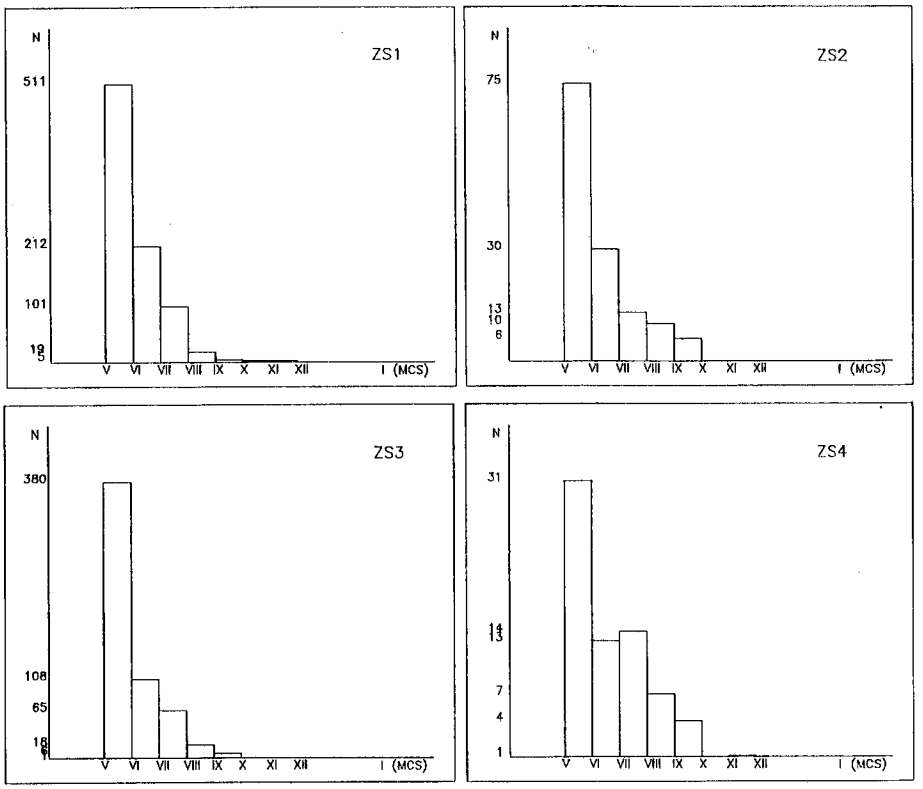

Fig. 6 - Histograms of the seismicity distribution for each source zone over 1000 years.

Previous studies on the attenuation coefficients, calculated with the Blake (1941), Howell and Schultz (1975) relations, simple exponential and Grandori (1987), for the investigated area (Pietrafesa ed al., 1990) have shown quite different values from those obtained using Sponheuer's model (adopted for uniformity with the model used in the program). A preliminary attempt was made by inserting into the input file the coefficients obtained with an esponential attenuation model derived from Blake's relation (Bottari ed al., 1979). As shown here for the parameters considered, in future we propose to further improve the methodology for the evaluation of influence of seismic attenuation on the intensity projection.

RESULTS

For each combination of input parameters employed, maps of the maximum expected intensities for return periods between 50 and 500 years were produced. The maps with return periods of 200 and 500 years were chosen and compared. The choice of maps with return period of 200 years was justified by the interval of completeness for the examined area: a projection of 200 years, on a basis of Catalogue completeness of 180 years, should have a good degree of affidability. The historical seismicity does not show appreciable differences for the maximum intensity over time periods longer than 180 years (eg. 300 years). This justified the choice of the return period of 500 years for an historical basis of 180 years. Moreover, projection values for return periods of 200 and 500 years have been understimated with respect to the historical values (XI MCS, earthquake of the Straits of Messina, December 28, 1908); therefore it was foreseen that by increasing the time period, the results would better approximate the observed historical values.

To represent the isolines, intervals of 0.2 MCS were chosen. Although intensity values which

are not integer or semi-integer do not have pratical significance and cannot be considered consistent with the criteria of the MCS scale, this step was taken in order to highlight the variations in shape of the isolines.

In order to show the influence of geometry and orientation of the source zones on the intensity projection, the maps for the various geometries considered were put together choosing the same combinations of assumed maximum intensities and uncertainties (Figs. 7-10). From a comparison of the groups of maps with return periods considered, it was possible to show that the reduction in size of source zones produces, for the conditions in Figs. 7 and 8, an increase in the maximum projection values of 4/10 degrees; for the conditions represented in Figs. 9 and 10, the increase was 2/10 degree. It was also noted how the different geometries and orientations of the source zones influence the "shape" of the isolines (which are always consistent with the geometry of the source zones) and the distribution of the projection intensity values, which are more noticeable in the sites around the limits of the same source zones. This can be seen by comparing, in particular, maps b and c of each figure, corresponding to the two configurations of the areally reduced source zones, and characterized by the two different orientations of ZS2. A different distribution of intensity is also to be noted, particularly evident in the area of Patti, more directly influenced by the variations of ZS2. A comparison of the maps corresponding to the same geometry of the source zones (parts a, b and c of Figs. 7 to 10) allows us to indicate the "weight" of the maximum intensity values assumed, and the relative uncertainty on the projection intensity. In particular, it can be pointed out that on assuming "exact" historical information, lower values are obtained for the intensity projection; on attribuing the value 0.5 to the standard deviation, an increase of 2/10 degree is obtained. On maintaining the conditions represented in Fig. 7 and by varying alternatively the two parameters, an increase in the maximum values of the projection intensity is also seen, quantifiable in 4/10 degrees for the intensities with return period of 200 years, and in 6/10 degree for those with return period of 500 years.

Fig. 11 shows the maps relative to the same geometry of the source zones, for the different assumed intensities and relative uncertainties (maintaining again the conditions of Fig. 7), obtained from a test carried out using different values of attenuation coefficients. It shows smaller variations in projection intensity, accompanied by a general increase in the areas delimited by each isoline, and indicating a different distribution of the maximum intensities expected throughout the area investigated. These last results are coherent with the introduction of attenuation coefficient values which are lower with respect to previous tests. We think, however, that a more detailed analysis should be carried out to establish the degree of influence of the "attenuation" parameter on the projection intensity.

CONCLUSIONS

The best results from an investigation of seismic hazard carried out in a fixed area are obtained from the minimization of errors in the projection of the maximum expected intensities. Care is therefore necessary in the composition of the input file to the calculation program employed. Moreover, a correct interpretation of the geologic-structural framework of the region is of great importance.

From these considerations, the utility of characterizing the "weight" of each input parameter becomes evident; in particular of those tied to subjective decisions in the valuation of the seismic hazard. Various tests were carried out for different combinations of input parameters characteristic of the source zones identified for the Calabro-Sicilian region.

With reference to the maps of maximum expected intensities, it is possible to link the variations of intensity with changes in the different input parameters. This allows the quantification of the "weight" of each of them in the seismic hazard evaluation.

From the tests carried out, it emerges how, in general, areal reduction of the source zones generates, as foreseeable, an increase in the projection intensity quantifiable in 4/10 degrees. Similar variations can be observed by varying the attenuation coefficients. The assumed values

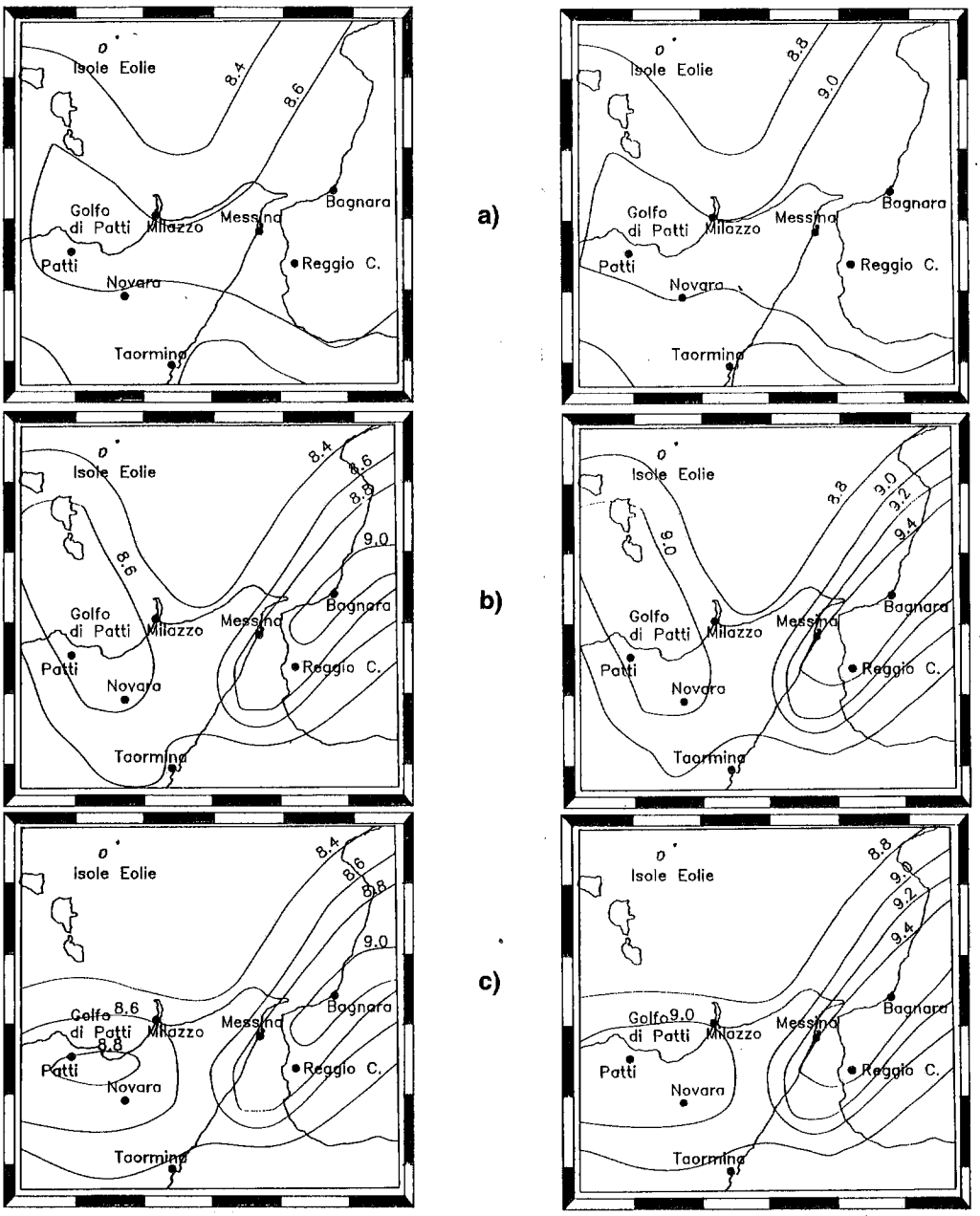

Fig. 7 - Map of the maximum expected intensities with a return period fo 200 years (left side) and 500 years (right side), $(I_{max})_{AS}=(I_{max})_{OS}$ and $\sigma=0.0$; for different configurations of the ZS: a) map for the ZS of Fig. 5a, b) map for the ZS of Fig. 5b, c) map for the ZS of Fig. 5c.

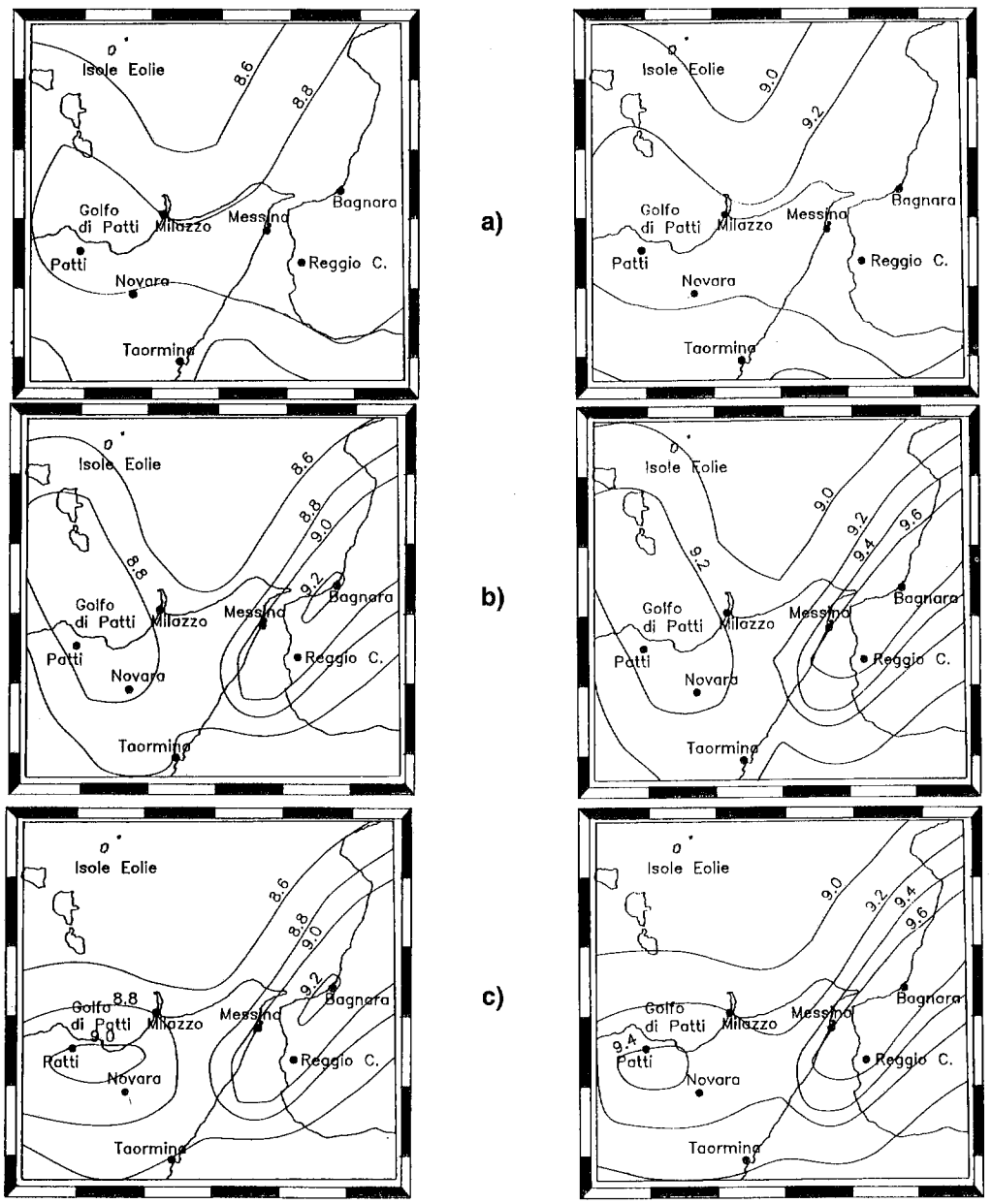

Fig. 8 - Map of the maximum expected intensities with a return period of 200 years (left side) and 500 years (right side), $(I_{max})_{AS}=(I_{max})_{OS}$ and $\sigma=0.5$; for different configurations of the ZS: a) map for the ZS of Fig. 5a, b) map for the ZS of Fig. 5b, c) map for the ZS of Fig. 5c.

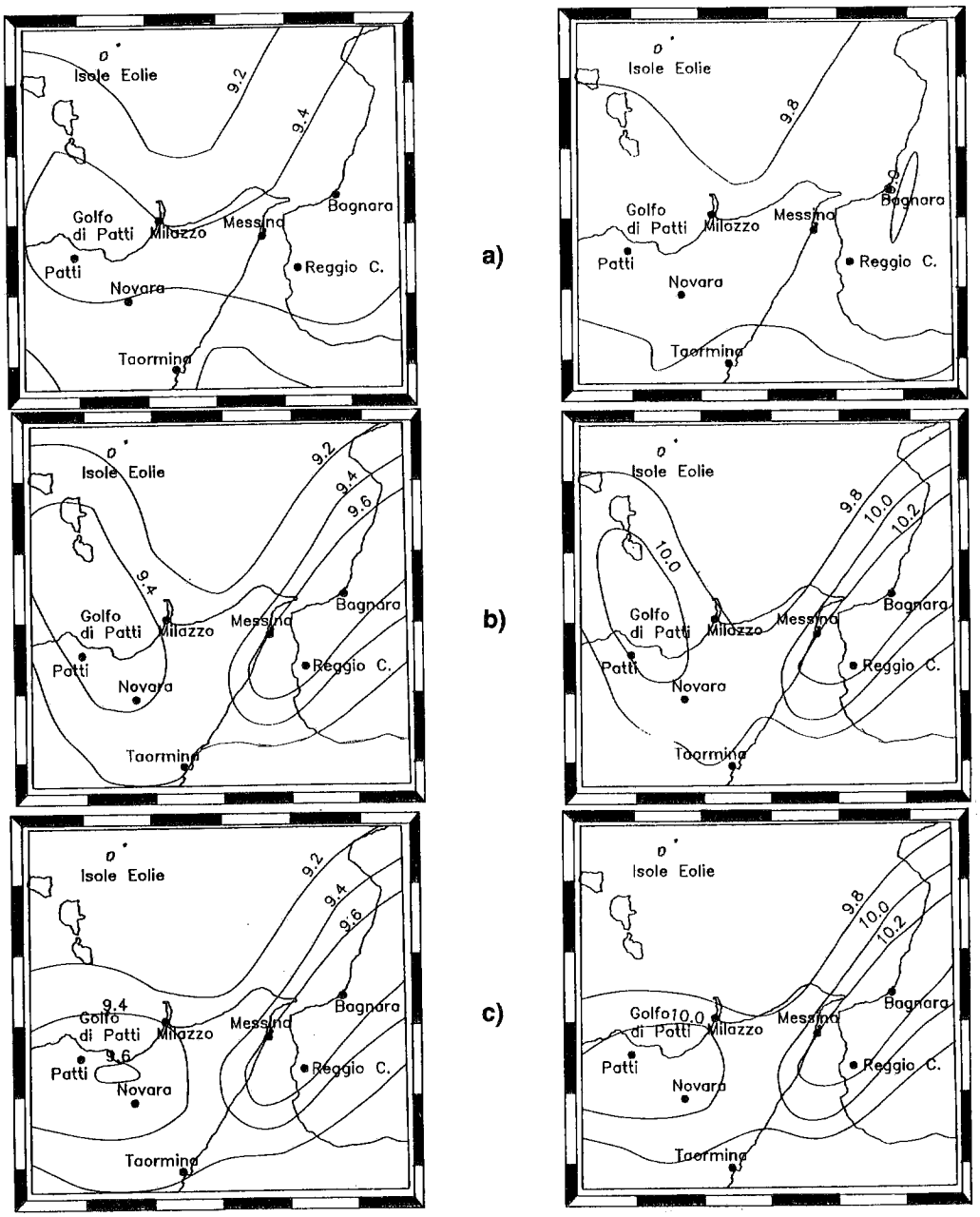

Fig. 9 - Map of the maximum expected intensities with a return period of 200 years (left side) and 500 years (right side), $(I_{max})_{AS} = (I_{max})_{OS}$ and $\sigma = 1.0$; for different configurations of the ZS: a) map for the ZS of Fig. 5a, b) map for the ZS of Fig. 5b, c) map for the ZS of Fig. 5c.

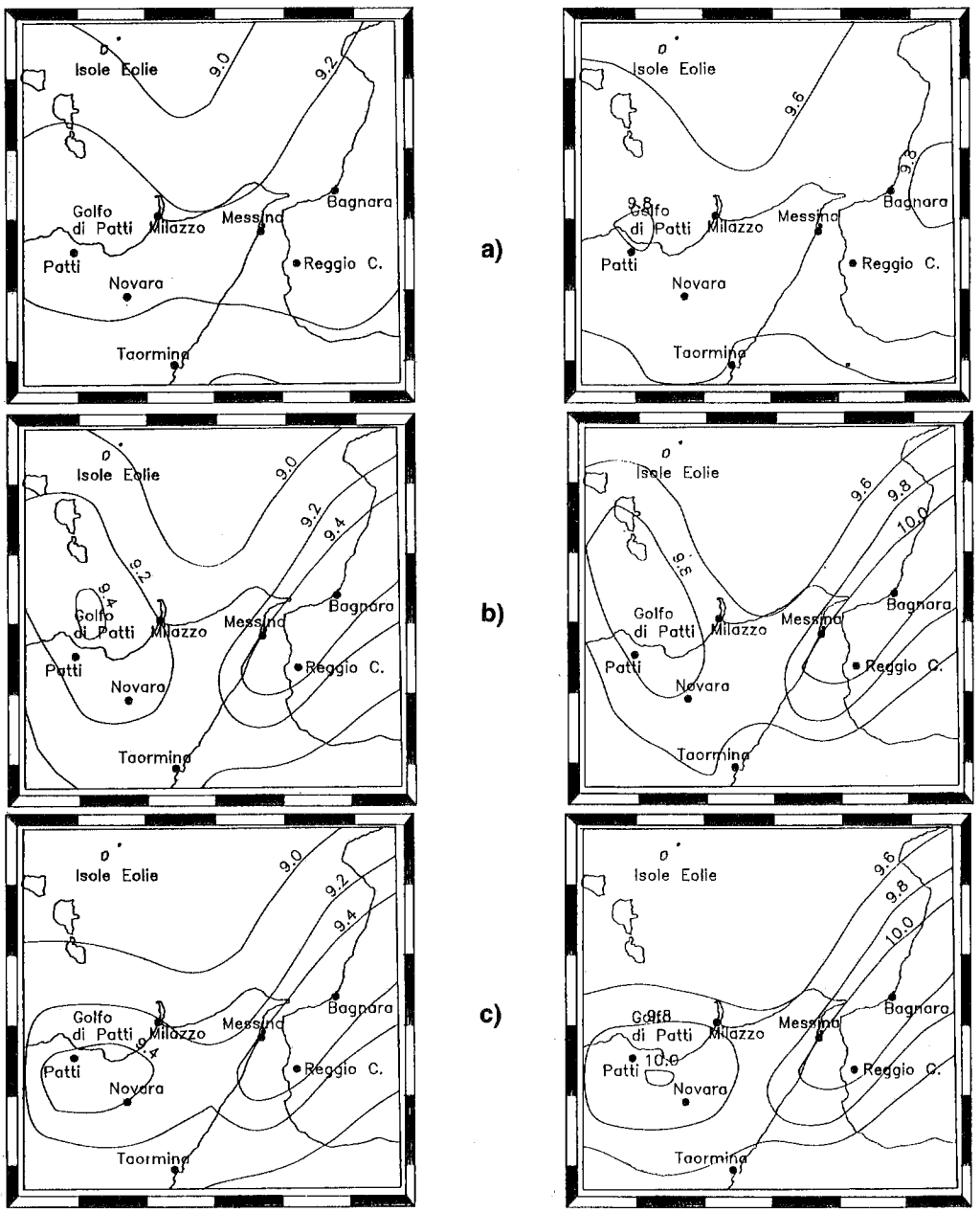

Fig. 10 - Map of the maximum expected intensities with a return period of 200 years (left side) and 500 years (right side), $(I_{max})_{AS}=(I_{max})_{OS}+1$ and $\sigma=0.5$; for different configurations of ZS: a) map for the ZS of Fig. 5a, b) map for the ZS of Fig. 5b, c) map for the ZS of Fig. 5c.

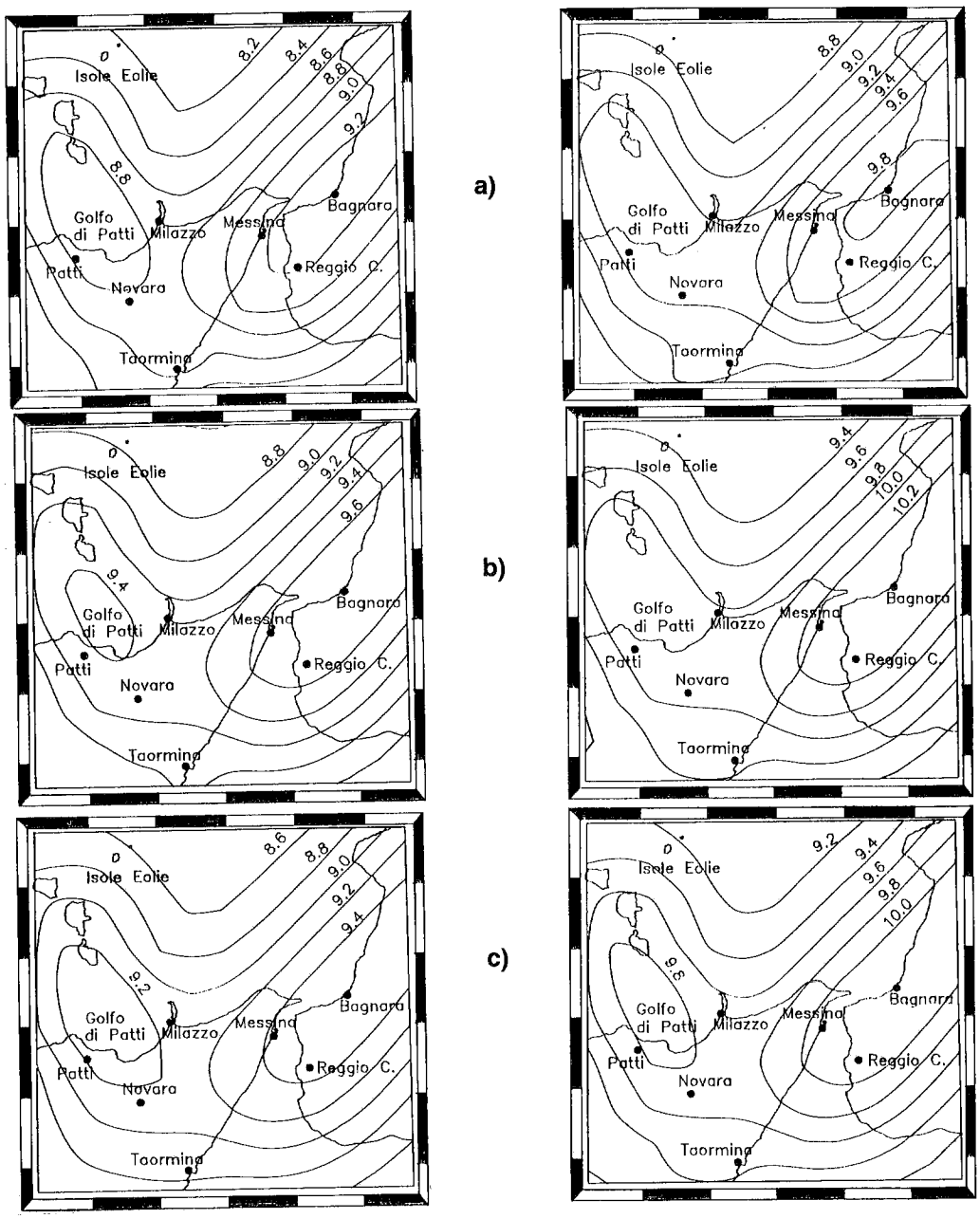

Fig. 11 - Map of the maximum expected intensities with a return period of 200 years (left side) and 500 years (right side) derived by varing the attenuation coefficients, for the configuration of the ZS of Fig. 5b and different intensity values of the largest possible earthquake and uncertainty: a) $(I_{max})_{AS}=(I_{max})_{OS}$ and $\sigma=0.5$, b) $(I_{max})_{AS}=(I_{max})_{OS}+1$ and $\sigma=0.5$, c) $(I_{max})_{AS}=(I_{max})_{OS}$ and $\sigma=1.0$.

for the historical intensities and the relative uncertainty generate, for a return period of 200 years, an increase on 4/10 degrees; more considerable is the increase in the intensity projection for a return period of 500 years, quantifiable in 6/10 degree. In general, from an analysis of the expected intensity maps, it is shown that the values of expected intensities are understimated at certain sites of the examined area; the undervaluation was greates for the 200 year projections with respect to those of 500 years. The expected intensity values obtained for Messina and Reggio Calabria can be considered as an example ($I_{max}=9.6$ MCS for $T=200$ years, $I_{max}=10.2$ MCS for $T=500$ years), and are respectively 1.4 MCS and 0.8 MCS lower than the historical maxima observed ($I_o=11$ MCS) relative to the earthquake of 28.12.1908). XI MCS, on the other hand, is the maximum historical intensity observed in this area for the millennium considered. Further studies are necessary, in our opinion, to decide whether at the origin of such differences are particular conditions of input (which are, as seen, extremely diverse) or whether there are limits inherent in the program relative particular calculation procedure used giving systematic discrepancies between the values of historical and expected seismicity.

REFERENCES

Barbano M.S., Bressan G. e Zonno G.; 1986: *Valutazione della pericolosità sismica di una zona compresa tra il Garda ed il Friuli: risultati e confronti.* Rapporto del Reparto Terremoti dell'Istituto per la Geofisica della Litosfera (Milano) per la linea di ricerca "Pericolosità Sismica", Ottobre 1986.

Barbano M.S., Colombo F. e Zonno G.; 1988: *Valutazione della pericolosità sismica nell'area del Sannio-Matese.* I: Atti del 7° Convegno G.N.G.T.S., Esagrafica, Roma, pp. 295-306.

Barbano M.A., Colombo F. and Zonno G.; 1989a: *Preliminary results of seismic hazard assessment in the Sannio-Matese area of Southern Italy.* Natural Hazard, **2**, 307-328.

Barbano M.S., Egozcue J.J., Garcia Fernandez M., Kijko A., Lapajne J., Mayer-Rosa D., Schenk V., Schenkova Z., Slejko D. and Zonno G.; 1989b: *Assesment of seismic hazard for the Sannio-Matese area of Southern Italy - A summary.* Natural Hazard, **2**, 217-228.

Bath M. and Duda S.J.; 1964: *Earthquake volume, fault plane area, seismic energy, strain, deformation and related quantities.* Ann. Geof., **17**, 353-361.

Blake A.; 1941: *On the estimation of focal depth from macroseismic data.* Bull. Seism. Soc. Am., **31**, 3-12.

Bottari A., Federico B. and Lo Giudice E.; 1979: *Methodological considerations regarding the determination of some macroseismic field parameters. Application to earthquakes in the Calabro-Peloritano Arc.* Boll. Geof. Teor. Appl., **21**, 197-225.

Ghisetti F. and Vezzani L.; 1982: *Different styles of deformation int he Calabrian arc (Southern Italy): implication for a seismotectonic zoning.* Tectonophysics, **85**, 149-165.

Grandori G., Perotti F. and Tagliani A.; 1987: *On the attenuation of macroseismic intensity with epicentral distance.* In: Cakmak A.S. (ed.), *Ground Motion and Engineering Seismology*, 3° Int. Conf. Soil Dynamics and Earthquake Engineering, Princeton, Elsevier, Amsterdam, pp. 581-594.

Howell B.F. jr. and Schultz T.R.; 1975: *Attenuation of modified Mercalli intensity with distance from epicenter.* Bull. Siesm. Soc. Am., **65**, 651-665.

McGuire R.; 1976: *Fortran computer program for seismic risk analysis.* U.S. Geological Survey, Open-file Report, 76-67.

Pietrafesa M., Teramo A., Cefali F. and Bottari A.; 1990: *A comparison of different attenuation models for macroseismic intensity.* Boll. Geof. Teor. Appl., **32**, 215-224.

Postpischl D. (ed); 1985: *Catalogo dei Terremoti Italiani dall'anno 1000 al 1980.* C.N.R./P.F.G., 114, 2B.

Saeggesser R. and Mayer-Rosa D., 1978: *Erdbebgefaehrdung in der Shweiz.* Schweis. Bauz, **98**,B 107-123.

Slejko D. and Siro L.; 1988: *On the seismic hazard of Southern Apennines.* In: Atti del 7° Convegno G.N.G.T.S., Esagrafica, Roma, pp. 191-202.

Siro L. and Slejko D.; 1989: *Different approaches to the seismic hazard of Sannio-Matese (Southern Italy).* Natural Hazard, **2**, 329-348.

Sponhewer W.; 1960: *Methoden Zur Herdtiefenbestimmung in der Makroseismic.* Freiburger Forsch. H., C88.